One-dimensional $\mathcal{PT}$-symmetric acoustic heterostructure

Hai-Xiao Zhang(张海啸)[1,2], Wei Xiong(熊威)[1], Ying Cheng(程营)[1,3,†], and Xiao-Jun Liu(刘晓峻)[1,3,‡]

[1] *Department of Physics, MOE Key Laboratory of Modern Acoustics, Collaborative Innovation Center of Advanced Microstructures, Nanjing University, Nanjing* 210093, *China*

[2] *School of Electrical and Information Engineering, Changzhou Institute of Technology, Changzhou* 213032, *China*

[3] *State Key Laboratory of Acoustics, Institute of Acoustics, Chinese Academy of Sciences, Beijing* 100190, *China*

(Received 5 August 2022; revised manuscript received 8 September 2022; accepted manuscript online 9 September 2022)

The explorations of parity–time ($\mathcal{PT}$)-symmetric acoustics have resided at the frontier in physics, and the pre-existing accessing of exceptional points typically depends on Fabry–Perot resonances of the coupling interlayer sandwiched between balanced gain and loss components. Nevertheless, the concise $\mathcal{PT}$-symmetric acoustic heterostructure, eliminating extra interactions caused by the interlayer, has not been researched in depth. Here we derive the generalized unitary relation for one-dimensional (1D) $\mathcal{PT}$-symmetric heterostructure of arbitrary complexity, and demonstrate four disparate patterns of anisotropic transmission resonances (ATRs) accompanied by corresponding spontaneous phase transitions. As a special case of ATR, the occasional bidirectional transmission resonance reconsolidates the ATR frequencies that split when waves incident from opposite directions, whose spatial profiles distinguish from a unitary structure. The derived theoretical relation can serve as a predominant signature for the presence of $\mathcal{PT}$ symmetry and $\mathcal{PT}$-symmetry-breaking transition, which may provide substantial support for the development of prototype devices with asymmetric acoustic responses.

Keywords: acoustic $\mathcal{PT}$-symmetric heterostructure, anisotropic transmission resonance, occasional bidirectional transmission resonance

PACS: 43.20.+g, 43.35.+d, 43.20.El, 43.20.Fn **DOI:** 10.1088/1674-1056/ac90b3

1. Introduction

One of the most intriguing developments in quantum mechanics over the past few decades has been the discovery of a non-Hermitian Hamiltonian $\mathcal{H}$ that commutes with the parity-time ($\mathcal{PT}$) operator, a property that leads to real-energy eigenvalues.[1–3] Recently, considerable efforts have been further motivated to investigate its classical analogy in photonics,[4–12] acoustics,[13–23] and many more areas[24–27] by means of interleaving balanced loss–gain regions. In contrast to the photonic gain that can be straightforwardly implemented in a locally controlled fashion through stimulated emission, which involves optical (electrical) pumping by an external source or via parametric processes,[28–31] no passive acoustic gain material exists in nature. General physical realizations of acoustic $\mathcal{PT}$ symmetry rely on the presence of electromechanical cone loudspeakers,[14–16] forced air flows,[17] or piezoelectric transducers.[19,20] Although the equivalent loss–gain balance can be circumvented by implementing unbalanced loss-only structures,[32,33] the absence of gain gives rise to the intrinsic loss of overall energy. More recently, the implementations of effective acoustic gain through electro-thermoacoustic[34–38] and photo-thermoacoustic[39,40] effects promise versatile routes for the exploration of acoustic $\mathcal{PT}$ symmetry.

Up to now, all available designs of $\mathcal{PT}$-symmetric acoustics are constructed on the basis of balanced gain-loss pair coupled by elaborately configured interlayer, which take advantage of additional coupling mechanism. For example, the unidirectional transmission resonance in Ref. [13] is induced by the $\mathcal{PT}$ symmetry and the Fabry–Perot (FP) resonance of the system. However, the bidirectional transmission resonance in Ref. [21] is the consequence of the $\mathcal{PT}$ symmetry, FP resonance, and periodic structure of the system. Thus, the presence of exceptional points is investigated by varying the distance d between the gain and loss components, and their balance is achieved for specific values of $k_0 d$, where k_0 stands for the wave number in air. Therefore, the concise heterostructure without interlayer impling entirely disparate physics and design philosophies to $\mathcal{PT}$ symmetry[9] urgently needs to be adequately exploited, according the degree of freedom of acoustic medium, geometry and frequency simultaneously via a generalized theoretical model.

The purpose of this article is to explore the specific properties when $\mathcal{PT}$ symmetry imposes on the transmission and reflection in arbitrarily $\mathcal{PT}$-symmetric heterostructure, in both the symmetric and broken-symmetric phases by using an experimental parameter-related transfer matrix in acoustics. We first derive the conservation relations governing the one-dimensional (1D) $\mathcal{PT}$-symmetric acoustic heterostructure, which could be employed to predominantly determine whether $\mathcal{PT}$ symmetry is achieved in a given physical structure. A set of transmission resonance patterns are demonstrated as a consequence of the derived conservation relations,

†Corresponding author. E-mail: chengying@nju.edu.cn
‡Corresponding author. E-mail: liuxiaojun@nju.edu.cn

© 2022 Chinese Physical Society and IOP Publishing Ltd

in which the reflection vanishes only for waves incident from one side of the structure, referred to as anisotropic transmission resonances (ATRs). Last, we demonstrate an occasional bidirectional transmission resonance (OBTR) with bidirectional transparency but vastly different spatial pressure profiles for incidence from opposite sides. The findings may provide substantial support for the development of $\mathcal{PT}$-symmetric theory and prototype devices with richer acoustic phenomena.

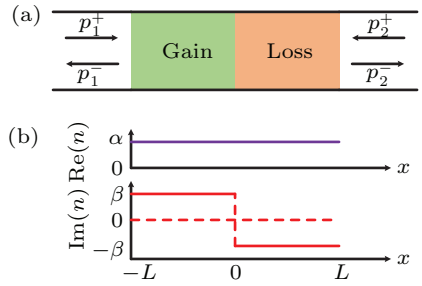


Fig. 1. (a) Schematic diagram of a 1D $\mathcal{PT}$-symmetric acoustic heterostructure, constructed by a pair of medium layers that are $\mathcal{PT}$-symmetric about $x = 0$, *i.e.*, $n(x) = n^*(-x)$ in panel (b). Green and orange regions indicate gain and loss medium, respectively.

2. Generalized unitary relation

We begin with the scattering matrix $S_{\rm r}$ defined by[17]

$$\begin{bmatrix} p_1^- \\ p_2^+ \end{bmatrix} = S_{\rm r} \begin{bmatrix} p_1^+ \\ p_2^- \end{bmatrix} \equiv \begin{bmatrix} r_{\rm G} & t \\ t & r_{\rm L} \end{bmatrix} \begin{bmatrix} p_1^+ \\ p_2^- \end{bmatrix}, \tag{1}$$

where $p_{1,2}^+$ and $p_{1,2}^-$ represent the sound pressure spreading along the forward and backward directions, respectively, with the subscript 1 (2) denotes the gain (loss) side, as illustrated in Fig. 1(a). $r_{\rm G}$ ($r_{\rm L}$) is the reflection coefficient from the gain (loss) side of the system, and t is the transmission coefficient from both sides. The subscript in $S_{\rm r}$ indicates that its diagonal elements are the reflection coefficients.

The overall transfer matrix $\Gamma = \Gamma_1\Gamma_2$ can be obtained,[41] where Γ_m is the transfer matrix expressed as

$$\Gamma_m = \begin{bmatrix} \cos(k_m L) & {\rm i}\sin(k_m L) Z_m \\ {\rm i}\sin(k_m L)/Z_m & \cos(k_m L) \end{bmatrix}. \tag{2}$$

Here $m = 1, 2$ denote the gain or loss components with length L. In $\mathcal{PT}$-symmetric acoustics, we have $k_m = k_0 n_m$ with k_m being the wave vector in the acoustic gain (loss) region. $n_m = \alpha \pm {\rm i}\beta$ is the refractive index of the gain (loss) region [see Fig. 1(b)], which can be obtained from the mass density ρ_m and bulk modulus κ_m of the gain (loss) component with $n_m = \sqrt{\kappa_0\rho_m/\rho_0\kappa_m}$. For the sake of simplicity, we assume that for the gain (loss) medium, the mass density is $\rho_m = \rho_0$ and the impedance is $Z_m = \sqrt{\kappa_0\rho_0}/n_m$, with ρ_0 and κ_0 being the mass density and bulk modulus of the air background.

Thus, the $S_{\rm r}$ matrix elements can be derived as

$$r_{\rm G} = {\rm i}a/\Delta, \quad r_{\rm L} = {\rm i}b/\Delta, \quad t = 2/\Delta, \tag{3}$$

where $\Delta = \delta_1 + {\rm i}\delta_2$, $a = \delta_3 + \delta_4$, $b = -\delta_3 + \delta_4$. After straightforward calculations and assuming $\xi = k_0 L$, we obtain

$$\begin{aligned} \delta_1 &= \frac{2}{N}\left[\alpha^2\cos(2\alpha\xi) + \beta^2\cosh(2\beta\xi)\right], \\ \delta_2 &= \frac{1}{N}\left[(1+N)\,\alpha\sin(2\alpha\xi) + (1-N)\,\beta\sinh(2\beta\xi)\right], \\ \delta_3 &= -\frac{P}{N}\left[\cos(2\alpha\xi) - \cosh(2\beta\xi)\right], \\ \delta_4 &= \frac{1}{N}\left[(1-N)\,\alpha\sin(2\alpha\xi) + (1+N)\,\beta\sinh(2\beta\xi)\right]. \end{aligned} \tag{4}$$

Here $N = \alpha^2 + \beta^2$; $P = 2\alpha\beta$; δ_1, δ_2, δ_3, δ_4, a and b are all real quantities.

Further calculation shows

$$ab = |\Delta|^2 - 4, \tag{5}$$

which gives the exact "generalized unitary relation"

$$r_{\rm G} r_{\rm L} = t^2\left(1 - \frac{1}{|t|^2}\right). \tag{6}$$

Equations (5) and (6) are valid for all 1D acoustic heterostructures with $\mathcal{PT}$ symmetry as following.

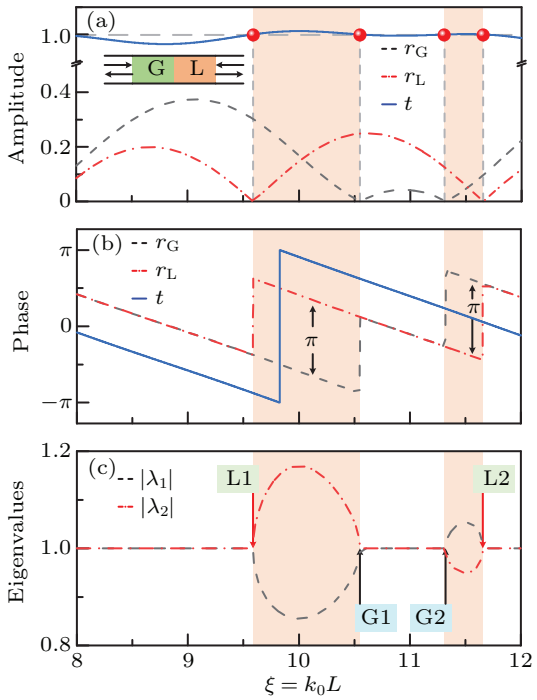


Fig. 2. (a) Reflection and transmission spectra of a 1D $\mathcal{PT}$-symmetric heterostructure with index $n = 0.8 \pm {\rm i}0.05$ and length L. The black dashed, red dashed-dotted, and blue solid curves show $|r_{\rm G}|$, $|r_{\rm L}|$, and $|t|$, respectively. Zeros of the reflections and corresponding anisotropic transmission resonances ($|t| = 1$) are marked by vertical gray dashed lines and red dots. (b) Phases of $r_{\rm G}$, $r_{\rm L}$, and t in panel (a), demonstrating the reflection phase jumps at each ATR. (c) Absolute eigenvalues of scattering matrix S_t. The four resonances marked as modes L1, G1, G2, and L2 from low to high frequency in sequence correspond to the reflection valleys in panel (a) and the phase jump points in panel (b). $|\lambda_1|$ and $|\lambda_2|$ are labeled and indicated by the black dashed and red dashed-dotted curves, respectively. The white and orange backgrounds indicate that the system is in the $\mathcal{PT}$-symmetric phase and broken phase, respectively.

For $|t| < 1$, we get $ab > 0$ from Eq. (5) and $|t|^2 + |r_{\rm G}||r_{\rm L}| = 1$ from Eq. (6). The former refers that $\varphi_{\rm G} =$

$\varphi_L = \varphi_t \pm \pi/2$, where $\varphi_{G,L}$, and φ_t are the phases of reflection and transmission coefficients. The latter is an intriguing generalization of the more familiar conservation relation $|t|^2 + |r|^2 = 1$, which applies to a unitary ($\mathcal{T}$-symmetric) matrix for which the left and right reflections (defined as r) are necessarily equal.[42] In the $\mathcal{PT}$-symmetric case, the geometric mean of the two reflectances $|r_G||r_L|$ replaces the single reflectance $|r|^2$. Therefore, when $|t| < 1$, the scattering of a single incident wave from one side of the structure is subunitary (some flux is lost) while the scattering from the other side is superunitary (some flux is gained). It should be noted that an accidental degeneracy only appears at $|r_G| = |r_L|$, in which case the flux conservation of scattering from both sides cannot be accomplished ($\delta_3 \neq 0$) unless an introducing additional tuning parameter (*e.g.*, the in-between air coupling layer in typical $\mathcal{PT}$-symmetric setup in Ref. [16]). The above mentioned phenomena are shown by the white background regions in Figs. 2(a) and 2(b), which describe the scattering properties of a 1D $\mathcal{PT}$-symmetric heterostructure with index $n = 0.8 \pm \mathrm{i}0.05$ and length L.

In contrast, when $|t| > 1$, all single-sided scattering processes are superunitary. Thus, we obtain $ab < 0$ from Eq. (5) and the conservation relation of Eq. (6) becomes $|t|^2 - |r_G||r_L| = 1$. Similarly, the former indicates that $\varphi_G - \varphi_L = \pi$ and $\varphi_{G,L} = \varphi_t \pm \pi/2$, while the latter describes a class of conservation relations that cannot exist in Hermitian systems. Accidental reflection degeneracies ($|r_G| = |r_L|$, requiring $\delta_4 = 0$) are possible in this regime,[42] leading to the usual pseudounitary conservation relation $|t|^2 - |r|^2 = 1$, as shown by the orange background in Figs. 2(a) and 2(b).

To further explore the $\mathcal{PT}$ symmetry of the structure, we consider the scattering matrix[13]

$$S_t = S_r\sigma_x = \begin{bmatrix} r_G & t \\ t & r_L \end{bmatrix} \begin{bmatrix} 0 & 1 \\ 1 & 0 \end{bmatrix} = \begin{bmatrix} t & r_G \\ r_L & t \end{bmatrix}, \tag{7}$$

where σ_x is one of the Pauli matrices and the subscript in S_t indicates that its diagonal elements are the transmission coefficients. The eigenvalues of S_t can be obtained as $\lambda_{1,2} = t \pm \sqrt{r_G r_L} = (2 \pm \mathrm{i}\sqrt{ab})/\Delta$. From this relation, we can conclude that when $|t| < 1$ ($ab > 0$), the eigenvalues are unimodular ($|\lambda_1| = |\lambda_2| = 1$) but nondegenerate ($\lambda_1 \neq \lambda_2$), and the acoustic structure is in the so-called symmetric phase. However, when $|t| > 1$ ($ab < 0$), the eigenvalues are nonunimodular ($|\lambda_1| = |\lambda_2|^{-1} \neq 1$) and the structure is in the broken phase, as shown in Fig. 2(c).

3. Anisotropic transmission resonance

As noted above, equation (6) implies an considerable interesting phenomenon: there exists a flux-conserving scattering process for incident waves if and only if $|t| = 1$, while only a single one of r_G or r_L vanishes. Such process can be referred as an ATR,[9] which is a generalization of the flux-conserving transmission resonances in unitary structures ($\beta = 0$, $|r| = 0$, and $|t| = 1$) independent of the incidence direction. These ATR modes are marked by red dots in Figs. 2(a) and 2(c) as modes L1, G1, G2, and L2 at $k_0L = 9.59$, 10.55, 11.32, and 11.66, respectively. It is convenient to distinguish these four modes: (i) Modes G1 and G2 are ATRs at the gain-side reflectionless state ($r_G = 0$) corresponding to the gain-side reflection phase jumps, whereas modes L1 and L2 are ATRs at loss-side reflectionless state ($r_L = 0$) associated with the loss-side reflection phase jumps. (ii) Modes G1 and L1 arise from a bidirectional transmission resonance (BTR) ($\beta = 0$, $\xi_0 = \mu\pi/2\alpha$, and μ is an odd number) of the unitary structure, while modes G2 and L2 arise from the other BTR of the unitary structure ($\beta = 0$, $\xi_0 = \mu\pi/2\alpha$, and μ is an even number).

A surprising property of ATRs is that their intensity profile is spatially symmetric. For a spatial profile $p(x)$ of a left- (right-) going transmission resonance, $p^*(-x)$ after a $\mathcal{PT}$ operation is also a left- (right-) going transmission resonance of the same structure. Since these two states occur at the same frequency, they must be identical (up to a phase ϕ) by the requirement of uniqueness:

$$p^*(-x) = \mathrm{e}^{\mathrm{i}\phi} p(x). \tag{8}$$

Hence, the amplitude satisfies $|p^*(-x)| = |p(x)|$. This is consistent with the intuitive expectation that to conserve flux, the acoustic energy must spend an equal amount of time on average in the loss and gain regions of the heterostructure. Except at the ATRs, intensities do exhibit asymmetry for bidirectional incidence, and in particular this is the case for a wave incident from the side with nonvanishing reflection.

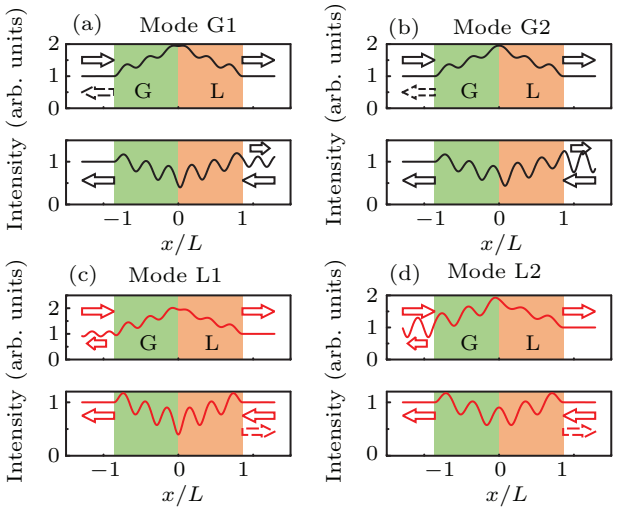


Fig. 3. (a)–(b) Spatial profiles of ATR modes G1 and G2, indicating unidirectional reflectionless from the gain side. (c)–(d) Spatial profiles of ATR modes L1 and L2, indicating unidirectional reflectionless from the loss side. The top (bottom) panel shows wave incidence from the gain (loss) side.

The spatial profiles of gain-side invisibilities, corresponding to the aforementioned ATRs of modes G1 and G2, are

shown in Figs. 3(a) and 3(b). The top panels exhibit the spatial symmetry of their pressure amplitude profile and the bottom panels identify the asymmetry under non-ATR condition. For comparison, figures 3(c) and 3(d) carry out a disparate vision of loss-side invisibilities, associated with the aforementioned ATRs of modes L1 and L2. To our surprise, in modes G1 and L1, the spatial profiles reach minimums at the gain–loss interface, which is consistent with the spatial profile of their corresponding BTR. As expected, modes G2 and L2 have a similar phenomenon, where the spatial profiles reach maximums at the gain-loss interface.

4. Occasional bidirectional transmission resonance

Owing to $\mathcal{PT}$ symmetry, a couple of ATRs therefore arise from the BTR of the unitary structure ($\beta = 0$), resulting in unidirectional invisibility at different frequencies and incident directions (*e.g.*, modes G1 and L1). Further exploration shows that, there exists a series of occasional bidirectional transmission resonances (OBTRs), which inherit the characteristic scattering properties of the unitary structure at a hand-to-hand frequency, but exhibit obvious differences in the amplitude profiles. The implementation of this phenomenon depends on the precondition of $a = b = 0$ ($\delta_3 = \delta_4 = 0$), which cannot be demonstrated strictly via the equation evolution. Nevertheless, this phenomenon can still be simulated under approximate conditions: (i) $\beta \ll \alpha$; (ii) $\beta\xi \sim 0$ (low normalized frequency); (iii) $\xi \sim \mu\pi/2\alpha$, and μ must be an even number; (iv) $\beta \sim 0$. We illustrate the mathematical and physical mechanisms that underline this phenomenon in detail.

According to the transfer matrix model, provided that the first three conditions are fulfilled, the scattering parameters can be reduced to

$$\delta_1 = 2, \quad \delta_2 = -\left(1 - \frac{1}{\alpha^2}\right)\beta(2\beta\xi),$$
$$\delta_3 = \frac{\beta}{\alpha}(2\beta\xi)^2, \quad \delta_4 = \left(1 + \frac{1}{\alpha^2}\right)\beta(2\beta\xi). \tag{9}$$

When $\beta \sim 0$, we obtain $\delta_2 \sim \delta_3 \sim \delta_4 \sim 0$, leading to $a \sim b \sim 0$ and $\Delta \sim 2$. Finally, $r_{\mathrm{G}} \sim r_{\mathrm{L}} \sim 0$, and $t \sim 1$. Otherwise, if $\xi = \mu\pi/2\alpha$ and μ is an odd number, the scattering parameters δ_2 and δ_4 remain the same, whereas δ_1 and δ_3 evolve into

$$\delta_1 = -2, \quad \delta_3 = \frac{\beta}{\alpha}\left[4 + (2\beta\xi)^2\right]. \tag{10}$$

It is much more complicated to implement an OBTR in the current case than in the previous case unless $4\beta/\alpha \sim 0$.

Based on the above four assumptions, we explore the scattering properties and spatial profiles of an OBTR in $\mathcal{PT}$-symmetric heterostructure and its mirrored BTR in a unitary structure. Figures 4(a)–4(c) show the scattering amplitudes, phases, and absolute eigenvalues of the $\mathcal{PT}$-symmetric heterostructure with index $n = 1.2 \pm \mathrm{i}0.05$, while figures 4(d)–4(f) exhibit the corresponding properties of unitary structure with index $n = 1.2$. Definitely, the OBTR shares an exceptional point (EP) with the initial BTR at $\xi = 2.64$ ($\sim \pi/\alpha$), however the scattering behavior near the EP is widely divergent. It is interesting to note that although the bidirectional reflection and transmission coefficients around EP are discrepant, the initial conservation relationship $|t|^2 + |r_{\mathrm{G}}||r_{\mathrm{L}}| = 1$ is still maintained, indicating that both structures undergo a symmetric phase [Figs. 4(a) and 4(d)]. This verdict can also be simply caught from the phases of scattering parameters, as shown in Figs. 4(b) and 4(e). Another point worth noting is that when OBTR occurs, the phase of the bidirectional transmission coefficient is $\varphi_t = 0$, which has never been demonstrated in a single $\mathcal{PT}$-symmetric structure but periodic cell units.[43,44] Whereas ATRs achieve unidirectional reflectionless (unitary transmission) in the $\mathcal{PT}$-symmetric heterostructure, OBTR approaches bidirectional invisibility, despite their acoustic pressure amplitude distribution in the gain-loss medium being different. Figure 4(c) shows the absolute eigenvalues of S_t for the $\mathcal{PT}$-symmetric structure, and there is a perturbation in the OBTR around the EP, which is consistent with the prediction that the OBTR is an approximate solution. On the contrary, for the unitary structure, the absolute eigenvalues are always one in the whole frequency range, as shown in Fig. 4(f).

Figures 4(g) and 4(h) demonstrate the spatial profiles of the EPs of mode "OBTR" in Fig. 4(c) and mode "BTR" in Fig. 4(f), respectively. The results indicate that both the $\mathcal{PT}$-symmetric heterostructure and the unitary structure exhibit unitary transmission at the unidirectional invisibility frequency, regardless of whether the incident wave initially passes through a waveguide with loss or gain. As shown in the top panel of Fig. 4(g), the incident wave with normalized frequency $\xi = 2.64$ passes through the gain portion from the left side, and the amplitude of the acoustic pressure increases to 1.118 (at the gain–loss interface). The amplitude then decreases to 1 in the loss portion. On the other hand, in the bottom panel of Fig. 4(g), the incident wave with identical normalized frequency first passes through the loss portion from the right side, and the amplitude of the acoustic wave decreases to 0.9 (at the loss–gain interface). The amplitude then increases to 1 in the gain portion. The spatially symmetric amplitude of acoustic waves indicates that the energy amplified (absorbed) in the gain (loss) waveguide is completely reproduced in the loss (gain) waveguide at the mirrored position, leading to unitary transmission and reflectionlessness.

This is distinct from the manifestation of the initial BTR in a unitary structure, in which the spatial profiles of bidirectional incidence are exactly reciprocal and the intensity at the gain–loss interface is undoubtedly 1 [Fig. 4(h)]. The conclusion further proves that OBTR in a $\mathcal{PT}$-symmetric heterostructure and BTR in unitary structure are two different physical processes, although their scattering matrices are identical, including amplitudes and phases.

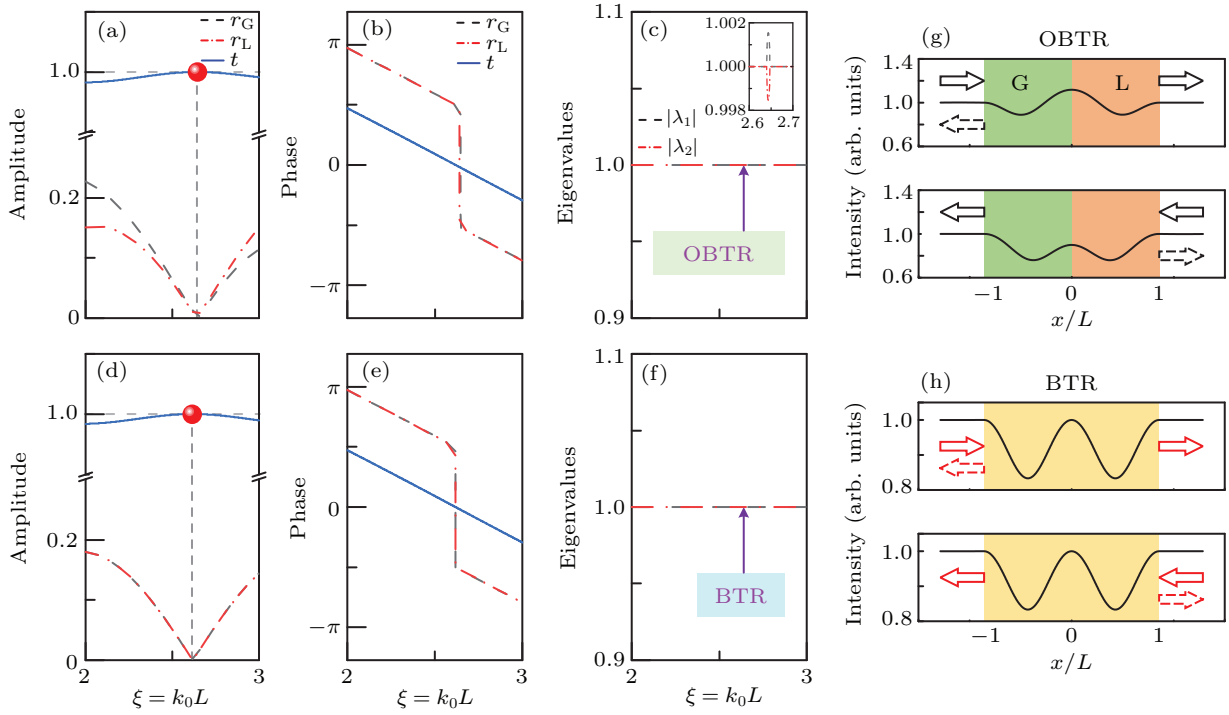


Fig. 4. (a) Reflection and transmission spectra of a 1D $\mathcal{PT}$-symmetric heterostructure with index $n = 1.2 \pm \mathrm{i}0.05$ and length L. Zero of the reflection corresponding to OBTR are marked by red dots. (b) Phases of r_{G}, r_{L}, and t in panel (a) demonstrate the reflection phase jump at EP. (c) Absolute eigenvalues of scattering matrix $\lambda_{1,2}$. The single mode marked as mode "OBTR" corresponds to the reflection valley in panel (a) and the phase jump point in panel (b). Inset: zoomed-in around the OBTR at $\xi = 2.64$. (d)–(f) Same as panels (a)–(c) but for unitary structure with index $n = 1.2$ and length $2L$. (g) The unitary nonrecopical transmission resonance of mode "OBTR" labeled in panel (c). (h) The profiles of mode "BTR" labeled in panel (f).

5. Conclusion and discussion

To conclude, we have derived the generalized unitary relation for the scattering matrix of arbitrary 1D $\mathcal{PT}$-symmetric acoustic heterostructure from the transfer matrix, including a conservation relation between the transmission and the gain (loss) side reflection. The conservation relation leads to a simple criterion for identifying the EPs at which the $\mathcal{PT}$ symmetry is spontaneously broken or restored. These EPs are shown to be closely related to the $\mathcal{PT}$-symmetry-breaking transition of the underlying effective Hamiltonian of the structure. In addition, the discovery of four patterns of ATRs has enhanced our physical understanding of $\mathcal{PT}$-symmetric heterostructure and its scattering EPs. The existence of the OBTR can also provide a theoretical basis for the realization of bidirectional transmission under non-Hermitian conditions and can be used as one of the methods of acoustic gain (loss) discrimination.

In practical realization, both types of components in the $\mathcal{PT}$-symmetric heterostructure can be realized by designing suitable circuits duo to the emergence of the active acoustic metamaterials,[14,16] which manifest the possibility of realizing the metamaterials with the required effective parameters. Our methodology can be applied to relevant fields such as electronics, optics, microwaves, and elastic metamaterials. Especially in recent years, preliminary studies have been made on $\mathcal{PT}$ symmetry in elastic wave system.[45–47] In view of the correlation between elastic and sound waves, elastic metamaterials may also provide potential ideas for experimental realization of acoustic $\mathcal{PT}$ symmetry, and *vice versa*. Our results are useful in predicting the propagation features of $\mathcal{PT}$-symmetric structures and designing devices of asymmetric responses.

Acknowledgements

Project supported by the National Basic Research Program of China (Grant No. 2017YFA0303702) and the National Natural Science Foundation of China (Grant Nos. 12225408, 12074183, 11922407, 11904035, 11834008, and 11874215).

References

[1] Bender C M and Boettcher S 1998 *Phys. Rev. Lett.* **80** 5243
[2] Bender C M, Boettcher S and Meisinger P N 1999 *J. Math. Phys.* **40** 2201
[3] Bender C M, Brody D C and Jones H F 2002 *Phys. Rev. Lett.* **89** 270401
[4] Mostafazadeh A 2009 *Phys. Rev. Lett.* **102** 220402
[5] Rüter C E, Makris K G, El-Ganainy R, Christodoulides D N, Segev M and Kip D 2010 *Nat. Phys.* **6** 192
[6] Longhi S 2010 *Phys. Rev. A* **82** 031801

[7] Chong Y, Ge L and Stone A D 2011 *Phys. Rev. Lett.* **106** 093902
[8] Lin Z, Ramezani H, Eichelkraut T, Kottos T, Cao H and Christodoulides D N 2011 *Phys. Rev. Lett.* **106** 213901
[9] Ge L, Chong Y and Stone A D 2012 *Phys. Rev. A* **85** 023802
[10] Feng L, Xu Y, Fegadolli W S, Lu M, Oliveira J E, Almeida Y R, Chen Y and Scherer A 2013 *Nat. Mater.* **12** 108
[11] Fleury R, Sounas D L and Alù A 2014 *Phys. Rev. Lett.* **113** 023903
[12] Wong Z J, Xu Y, Kim J, O'Brien K, Wang Y, Feng L and Zhang X 2016 *Nat. Photon.* **10** 796
[13] Zhu X, Ramezani H, Shi C, Zhu J and Zhang X 2014 *Phys. Rev. X* **4** 031042
[14] Fleury R, Sounas D L and Alù A 2015 *Nat. Commun.* **6** 5905
[15] Fleury R, Sounas D L and Alù A 2016 *IEEE J. Sel. Top. Quant.* **22** 121
[16] Shi C, Dubois M, Chen Y, Cheng L, Ramezani H, Wang Y and Zhang X 2016 *Nat. Commun.* **7** 11110
[17] Aurégan Y and Pagneux V 2017 *Phys. Rev. Lett.* **118** 174301
[18] Achilleos V, Aurégan Y and Pagneux V 2017 *Phys. Rev. Lett.* **119** 243904
[19] Hou Z and Assouar B 2018 *J. Appl. Phys.* **123** 085101
[20] Christensen J, Willatzen M, Velasco V and Lu M 2016 *Phys. Rev. Lett.* **116** 207601
[21] Ji W, Wei Q, Zhu X, Wu D and Liu X 2019 *Europhys. Lett.* **125** 58002
[22] Zhang H, Liu X, Bao Y, Zhang Y and Zhao J 2022 *Symmetry* **14** 965
[23] Zhang H, Zhang Y, Liu X, Bao Y and Zhao J 2022 *AIP Adv.* **12** 065217
[24] Schindler J, Li A, Zheng M C, Ellis F M and Kottos T 2011 *Phys. Rev. A* **84** 040101
[25] Zhou J, Zhang B, Xiao W, Qiu D and Chen Y 2018 *IEEE T. Ind. Electron.* **66** 4097
[26] Xiao Z, Rádi Y, Tretyakov S and Alù A 2019 *Research* **2019** 7108494
[27] Li Y, Peng Y, Han L, Miri M A, Li W, Xiao M, Zhu X, Zhao J, Alù A, Fan S and Qiu C 2019 *Science* **364** 170
[28] El-Ganainy R, Makris K G, Khajavikhan M, Musslimani Z H, Rotter S and Christodoulides D N 2018 *Nat. Phys.* **14** 11
[29] Özdemir Ş K, Rotter S, Nori F and Yang L 2019 *Nat. Mater.* **18** 783
[30] Klauck F, Teuber L, Ornigotti M, Heinrich M, Scheel S and Szameit A 2019 *Nat. Photon.* **13** 883
[31] Miri M A and Alù A 2019 *Science* **363** eaar7709
[32] Shen C, Li J, Peng X and Cummer S A 2018 *Phys. Rev. Mater.* **2** 125203
[33] Liu T, Zhu X, Chen F, Liang S and Zhu J 2018 *Phys. Rev. Lett.* **120** 124502
[34] Xiao L, Chen Z, Feng C, Liu L, Bai Z, Wang Y, Qian L, Zhang Y, Li Q, Jiang K and Fan S 2008 *Nano Lett.* **8** 4539
[35] Suzuki K, Sakakibara S, Okada M, Neo Y, Mimura H, Inoue Y and Murata T 2011 *Jpn. J. Appl. Phys.* **50** 01BJ10
[36] Suk J W, Kirk K, Hao Y, Hall N A and Ruoff R S 2012 *Adv. Mater.* **24** 6342
[37] BarnardA R, Jenkins D M, Brungart T A, McDevitt T M and Kline B L 2013 *J. Acoust. Soc. Am.* **134** EL276
[38] Hu B, Zhang Z, Zhang H, Zheng L, Xiong W, Yue Z, Wang X, Xu J, Cheng Y, Liu X and Christensen J 2021 *Nature* **597** 655
[39] Tian Y, Tian H, Wu Y, Zhu L, Tao L, Zhang W, Shu Y, Xie D, Yang Y, Wei Z, Lu X, Ren T, Shih C and Zhao J 2015 *Sci. Rep.* **5** 10582
[40] Giorgianni F, Vicario C, Shalaby M, Tenuzzo L D, Marcelli A, Zhang T, Zhao K, Chen Y, Hauri C and Lupi S 2018 *Adv. Funct. Mater.* **28** 1702652
[41] Pozar D M 2011 *Microwave engineering*, 4th edn. (John Wiley & sons) p. 190
[42] Jin L 2018 *Phys. Rev. A* **98** 022117
[43] Longhi S 2011 *J. Phys. A: Math. Theor.* **44** 485302
[44] Wu H, Yang X, Deng D and Liu H 2019 *Phys. Rev. A* **100** 033832
[45] Hou Z, Ni H and Assouar B 2018 *Phys. Rev. Appl.* **10** 044071
[46] Wu Q, Chen Y and Huang G 2019 *J. Acoust. Soc. Am.* **146** 850
[47] Farhat M, Chen P, Guenneau S and Wu Y 2021 *Phys. Rev. B* **103** 134101